NOX2 Deficiency Protects Against Streptozotocin-Induced β-Cell Destruction and Development of Diabetes in Mice

Fu-Li Xiang, Xiangru Lu, Brenda Strutt, David J. Hill, and Qingping Feng

OBJECTIVE—The role of NOX2-containing NADPH oxidase in the development of diabetes is not fully understood. We hypothesized that NOX2 deficiency decreases reactive oxygen species (ROS) production and immune response and protects against streptozotocin (STZ)-induced β-cell destruction and development of diabetes in mice.

RESEARCH DESIGN AND METHODS—Five groups of mice—wild-type (WT), $NOX2^{-/-}$, WT treated with apocynin, and WT adoptively transferred with $NOX2^{-/-}$ or WT splenocytes—were treated with multiple-low-dose STZ. Blood glucose and insulin levels were monitored, and an intraperitoneal glucose tolerance test was performed. Isolated WT and $NOX2^{-/-}$ pancreatic islets were treated with cytokines for 48 h.

RESULTS—Significantly lower blood glucose levels, higher insulin levels, and better glucose tolerance was observed in $NOX2^{-/-}$ mice and in WT mice adoptively transferred with $NOX2^{-/-}$ splenocytes compared with the respective control groups after STZ treatment. Compared with WT, β-cell apoptosis, as determined by TUNEL staining, and insulitis were significantly decreased, whereas β-cell mass was significantly increased in $NOX2^{-/-}$ mice. In response to cytokine stimulation, ROS production was significantly decreased, and insulin secretion was preserved in $NOX2^{-/-}$ compared with WT islets. Furthermore, proinflammatory cytokine release induced by concanavalin A was significantly decreased in $NOX2^{-/-}$ compared with WT splenocytes.

CONCLUSIONS—NOX2 deficiency decreases β-cell destruction and preserves islet function in STZ-induced diabetes by reducing ROS production, immune response, and β-cell apoptosis. ***Diabetes*** **59:2603–2611, 2010**

Type 1 diabetes is a T-cell–mediated autoimmune disease characterized by the selective destruction of insulin-secreting β-cells in the islets of Langerhans. It is a multifactorial process involving autoantigen presentation by macrophages, dentritic cells, and B-cells; activation of autoreactive $CD4^+$ T-cells; and activation and recruitment of β-cell–specific $CD8^+$ T-cells, leading to increased cytokine and reactive oxygen species (ROS) production and destruction of β-cells (1). The mechanisms of putative type 1 diabetes induced by multiple-low-dose streptozotocin (STZ) includes the direct β-cell destruction, which is mainly induced via DNA alkylation (2) and the indirect β-cell destruction from T-cell–dependent immune reaction (3). Furthermore, in response to cytokine stimulation including interleukin (IL)-1β, interferon (IFN)-γ, and tumor necrosis factor (TNF)-α, β-cells also generate ROS and reactive nitrogen species, which may facilitate their destruction (4). Additionally, overexpression of antioxidant enzymes including superoxide dismutase (SOD), catalase, and glutathione peroxidase 1 (Gpx1) protects against the onset and development of diabetes and supports an important role of ROS in the pathogenesis of immune-mediated diabetes (5–12). NADPH oxidase is one of the main sources of superoxide radical formation in many cell types including phagocyte and β-cells (13). This ROS-producing enzyme consists of two membrane subunits (NOX2 and $p22^{phox}$) and at least four cytosolic components ($p40^{phox}$, $p47^{phox}$, $p67^{phox}$, and Rac1). NADPH oxidase is a highly regulated enzyme. In the resting cells, the cytosolic complex is separated from the membrane-bound catalytic core. Upon stimulation, the cytosolic component $p47^{phox}$ becomes phosphorylated and the cytosolic complex migrates and binds to the membrane subunits to assemble into an active oxidase (14). It catalyzes the reduction of oxygen to superoxide anion using NADPH as a substrate and plays a major role in antimicrobial host defense as well as in tissue damage of autoimmune diseases (15,16). NOX2 is one of the critical subunits of NADPH oxidase. T-cells deficient in NOX2 exhibit an impaired ability to produce superoxide in response to anti-CD3 stimulation (17). Furthermore, glucose stimulates β-cell superoxide production, which can be inhibited by a selective NADPH oxidase inhibitor diphenylene iodonium, suggesting a functional NADPH oxidase in the islet (18). However, a definitive role of NADPH oxidase in the development of diabetes remains to be determined.

In the present study, $NOX2^{-/-}$ mice were used to investigate the role of NADPH oxidase in β-cell destruction induced by multiple-low-dose STZ. We demonstrated that NOX2 deficiency attenuates the severity of hyperglycemia and the loss of β-cell mass induced by STZ treatments via reduced ROS production and suppressed immune response.

RESEARCH DESIGN AND METHODS

Animals. $NOX2^{-/-}$ and C57BL/6 (wild-type [WT]) mice were obtained from Jackson Laboratory (Bar Harbor, ME). Male $NOX2^{-/-}$ and WT mice 8–12 weeks old were used in all experiments. Animals in this study were handled in accordance with the *Guide for the Care and Use of Laboratory Animals*, published by the U.S. National Institutes of Health (NIH publ. no. 85-23, revised 1996).

Adoptive transfer. Single-cell suspensions were prepared from spleens of $NOX2^{-/-}$ and WT mice as previously described (19). Briefly, spleens were removed, minced, and filtered through sterile 100-μm filters. Erythrocytes were lysed, and the nucleated cells were washed resuspended in saline and injected via the lateral tail vein into irradiated (970 cGy) WT mice (10^7

From the Departments of Medicine, Physiology, and Pharmacology, University of Western Ontario, Lawson Health Research Institute, London, Ontario, Canada.

Corresponding author: Qingping Feng, qfeng@uwo.ca.

Received 22 October 2009 and accepted 8 July 2010. Published ahead of print at http://diabetes.diabetesjournals.org on 13 July 2010. DOI: 10.2337/db09-1562.

cell/mouse). Mice that received NOX2$^{-/-}$ and WT splenocytes were termed WT$^{NOX2-/-}$ and WT^{WT}, respectively. These mice were allowed to recover for 5 weeks before the induction of diabetes.

Streptozotocin diabetes model. To induce diabetes, WT, NOX2$^{-/-}$, WT treated with apocynin (10 mg/day/kg body wt i.p.), WT$^{NOX2-/-}$, and WT^{WT} mice were treated with STZ (80 mg/kg body wt i.p. for 3 consecutive days). Additionally, some WT, NOX2$^{-/-}$ mice were treated with saline as vehicle controls. Random blood glucose levels were monitored on day 2, 5, and 8 after the final injection of STZ with a glucose meter (OneTouch Ultra2; LifeScan Canada, Burnaby, BC). On day 9, an intraperitoneal glucose tolerance test (IPGTT) was performed using an intraperitoneal injection of D-glucose at 2 g/kg body wt after 16 h fasting. Blood glucose was analyzed at 0, 15, 30, 60, and 120 min after introducing glucose. Nonfasting serum was collected. Pancreata were weighed and collected. Diabetic hyperglycemia was defined as a nonfasting blood glucose concentration >11.1 mmol/l for two or more consecutive tests.

Alloxan diabetes model. WT, NOX2$^{-/-}$ mice were treated with alloxan (60 mg/kg body wt i.v.). Fasting blood glucose levels were measured, and IPGTT was performed as described above. Nonfasting serum was collected for measurement of insulin levels.

Measurement of β-cell and islet mass, insulitis, and apoptosis. Pancreata from WT and NOX2$^{-/-}$ mice killed on day 9 were fixed in 4% paraformaldehyde for 24 h, embedded in paraffin, and serially cut into 5-μm sections at 50-μm intervals. Immunostaining was performed with an anti-mouse insulin antibody (1:2,000; Sigma, Oakville, ON) using a mouse-on-mouse immunodetection kit (Vector Laboratories, Burlingame, CA). The staining was visualized using diaminobenzidine. Sections were then counterstained with hematoxylin. The microscopic images were taken by a Zeiss microscope and analyzed using AxioVision software. Insulin-positive cells were considered functional β-cells. Relative β-cell and islet area to total pancreatic area ratios were calculated. The β-cell and islet mass were then evaluated by multiplying the area ratio with the pancreatic weight. The evaluation of insulitis score was assigned using the following scale: 0, intact islet; 1, peri-insulitis; 2, moderate insulitis (<50% of the islet infiltrated); and 3, severe insulitis (≥50% of the islet infiltrated) as previously described (19). For the analysis of pancreatic islet apoptosis, double staining of in situ cell death detection fluorescein and insulin fluorescent immunohistochemistry (20) was performed. Pancreata from WT and NOX2$^{-/-}$ mice killed 8 h after the final injection of STZ were isolated, embedded, and sectioned as described above. Apoptosis and necrosis of the islet cells were assessed via hematoxylin staining by the chromatin morphology (21).

Islet culture and treatment. Pancreatic islets were isolated from NOX2$^{-/-}$ and WT mice by liberase RI (Roche Diagnostics, Laval, QC) digestion as described previously (22). Isolated pancreatic islets were cultured free-floating in RPMI-1640 medium containing 11.1 mmol/l glucose, supplemented with 2 mmol/l L-glutamine, 10% FCS, 12 mmol/l HEPES, 100 units/ml penicillin, and 100 μg/ml streptomycin in an atmosphere of 95% air and 5% CO_2 at 37°C overnight. Groups of 20 islets were then incubated in 200 μl Dulbecco's modified Eagle's medium containing 11.1 mmol/l glucose supplemented with 2 mmol/l L-glutamine, 10% FCS, 100 units/ml penicillin, and 100 μg/ml streptomycin with or without a cytokine mixture, which consisted of human recombinant IL-1β, IFN-γ, and TNF-α (2 ng/ml each; Sigma) for 48 h at 37°C in 5% CO_2.

Determination of glucose-stimulated insulin release. The insulin secretion assay was performed as previously described (23). Briefly, islets from each experiment group were incubated in Krebs-Ringer bicarbonate buffer supplemented with 2 mg/ml BSA and 1.67 mmol/l glucose for 30 min, followed by a 90-min incubation in Krebs-Ringer bicarbonate HEPES buffer supplemented with 2 mg/ml BSA and in the presence of 1.67 or 16.7 mmol/l glucose. Insulin released during the 90 min was then measured and normalized by the DNA content of each 20-islet group. DNA content was determined by a CyQUANT-cell proliferation assay kit (Invitrogen Canada, Burlington, ON).

Detection of total ROS and superoxide production. Total ROS production in isolated islets was determined by dichlorofluorescein diacetate assay. Islets were homogenized in 100 μl buffer solution (50 mmol/l Tris-HCl, pH 7.5, 50 mmol/l KCl, and 10 mmol/l $MgCl_2$) and incubated with 10 μmol/l dichlorofluorescein diacetate at 37°C for 3 h. Fluorescence was measured by excitation (485 nm) and emission (525 nm) spectra with a microplate reader (SpectraMax M5; Molecular Devices, Sunnyvale, CA). Superoxide production in serum and isolated islets was determined by dihydroethidium assay. Serum and islets were incubated with 50 μmol/l dihydroethidium at 37°C for 30 min. Fluorescence was measured by excitation (396 nm) and emission (579 nm) spectra, which detects 2-hydroxyethidium (a specific superoxide-derived dihydroethidium product) (24), using a microplate reader (SpectraMax M5). Superoxide production in splenocytes in response to concanavalin A (ConA) was measured by lucigenin assay (25). Briefly, 10^6 splenocytes were treated with ConA (5 μg/ml) with or without

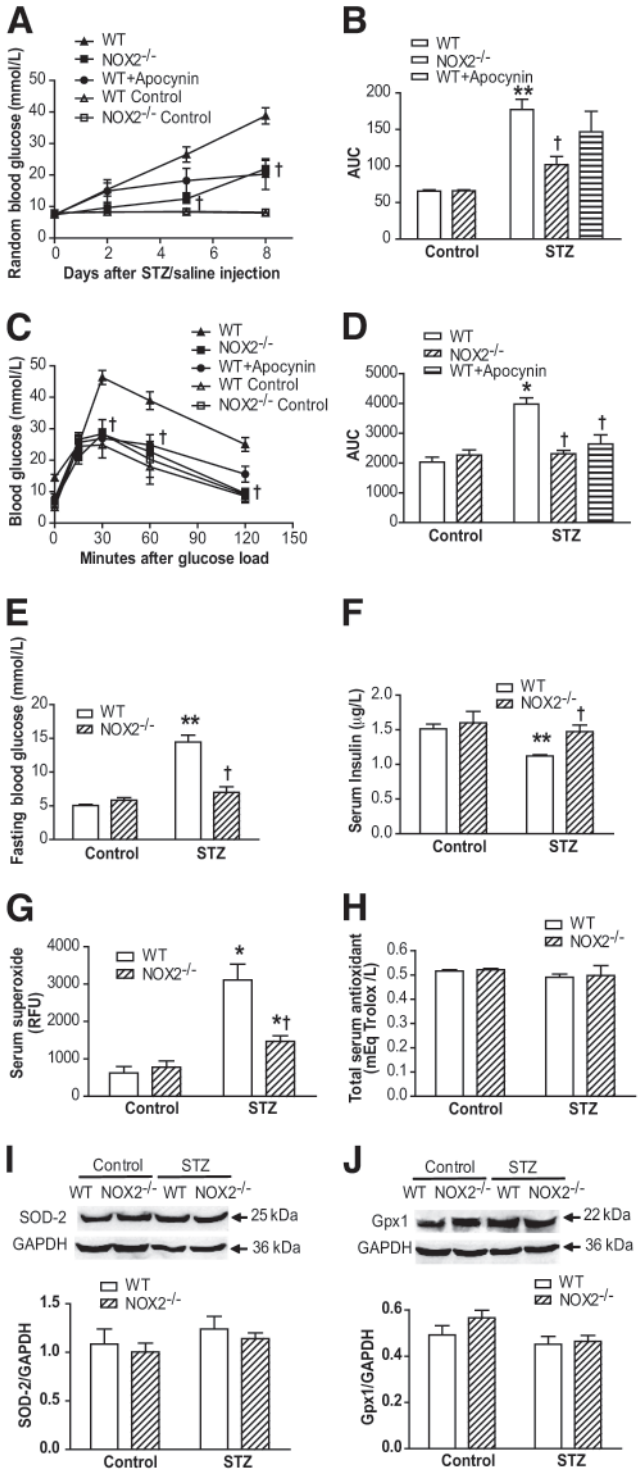

FIG. 1. Blood glucose and serum insulin levels after multiple-low-dose STZ treatment. *A* and *B*: NOX2$^{-/-}$ mice and WT mice treated with apocynin (10 mg/kg body wt/day) showed a significant decrease in random blood glucose levels compared with WT after STZ treatment. *C* and *D*: An IPGTT 9 days after STZ treatment revealed that glucose clearance was significantly improved in NOX2$^{-/-}$ and in WT mice treated with apocynin, compared with WT mice. *E*: NOX2$^{-/-}$ mice had a significantly lower fasting blood glucose level than WT mice after STZ treatment. *F–H*: After STZ treatment, serum insulin levels (*F*) in NOX2$^{-/-}$ mice were significantly higher, and superoxide levels (*G*) were significantly lower than those in WT mice. No difference in blood glucose and serum insulin was found between control groups. Total antioxidant levels, SOD-2, and Gpx1 expression was similar between WT and NOX2$^{-/-}$ mice (*H–J*). Data are means ± SEM, n = 6–7 per group for *A–H*, n = 4–5 per group for *I* and *J*. *P < 0.05, **P < 0.01 vs. WT control, †P < 0.05 vs. STZ-treated WT. AUC, area under the curve; RFU, relative fluorescence unit.

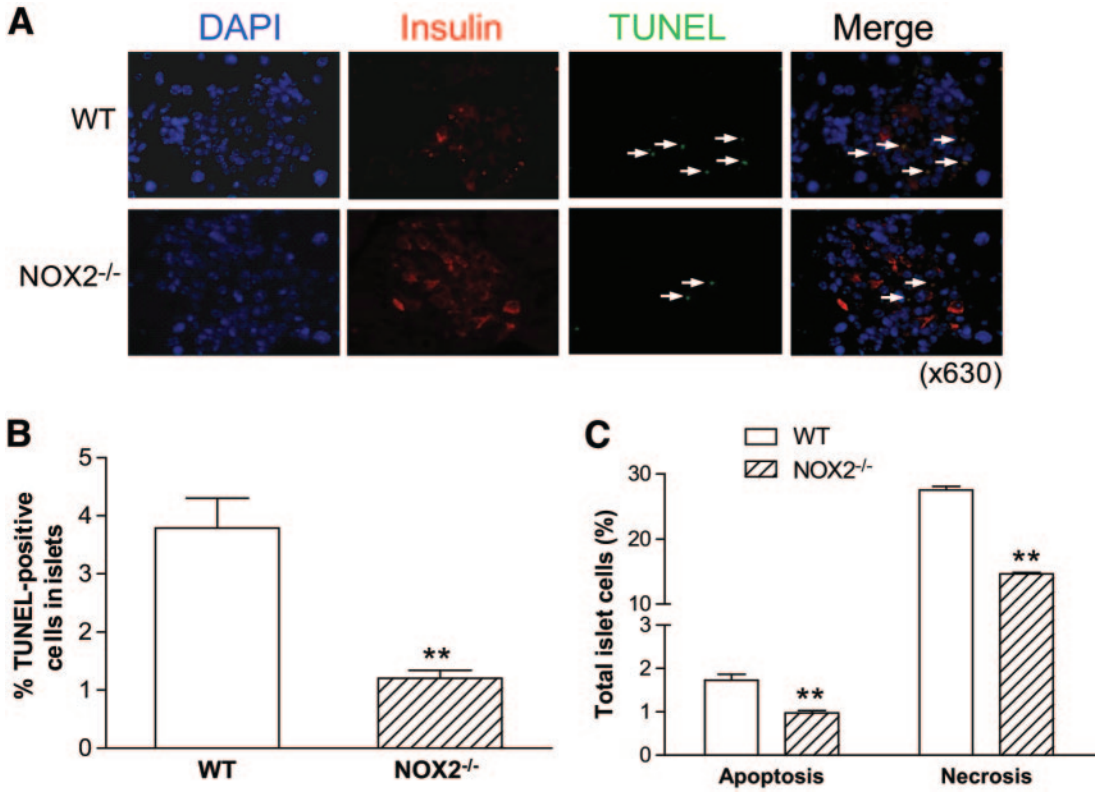

FIG. 2. Islet cell apoptosis after multiple-low-dose STZ treatment. *A*: Representative histological TUNEL staining of WT and NOX2$^{-/-}$ mouse islets 9 days after STZ treatment. *B*: STZ-induced β-cell apoptosis was significantly decreased in NOX2$^{-/-}$ compared with WT mice 9 days after STZ treatment. *C*: STZ-induced islet cell apoptosis and necrosis were both significantly decreased in NOX2$^{-/-}$ compared with WT mice directly after STZ treatment for 3 days. Data are means ± SEM, n = 5–7 per group. **P < 0.01 vs. STZ-treated WT. (A high-quality digital representation of this figure is available in the online issue.)

0.1 μmol/l diphenylene iodonium (NADPH inhibitor) for 5 min at 37°C followed by 50 μmol/l lucigenin. Luminescence was then measured using a microplate reader (SpectraMax M5).

Determination of cytokine release from splenocytes. Isolated splenocytes (5×10^6) from WT and NOX2$^{-/-}$ mice were cultured overnight and then incubated with ConA (5 μg/ml) for 48 h. TNF-α and IL-1β release in the media was determined by an ELISA kit (eBioscience, San Diego, CA).

Measurement of serum insulin and total antioxidant levels. Culture media of isolated islets in response to a 90-min stimulation of 1.67 and 16.7 mmol/l glucose were collected. Serum from nonfasting mice was obtained. Both culture media and serum were stored in −20°C, and their insulin concentrations were measured by a mouse insulin ELISA kit (ALPCO, Salem, NH). Serum insulin levels were expressed as micrograms per liter. Insulin concentrations in the culture media were adjusted by DNA content of the islets and expressed as nanograms per 100 μg islet DNA per 90 min. Serum total antioxidant levels were detected by a total antioxidant capacity assay kit (Abcam, Cambridge, MA) and were expressed as milliequivalents per liter of Trolox per liter (mEq Trolox/l).

Western blot analysis. Antioxidant enzymes manganese SOD (SOD-2) and Gpx1 protein levels were assessed by Western blotting. Briefly, cell lysates containing 80 μg protein were subjected to sodium dodecyl sulfate–PAGE using 12% gels, followed by electrotransfer to nitrocellulose membranes. Blots were probed with antibodies against SOD-2 (1:1,000; Santa Cruz Biotechnology, Santa Cruz, CA), Gpx1 (1:500; Abcam, MA), and GAPDH (1:8,000; Santa Cruz Biotechnology) followed by incubation with horseradish peroxidase–conjugated secondary antibodies (1:2,000; Santa Cruz Biotechnology). Protein bands were detected using the enhanced chemiluminescence method.

Statistical analysis. Data are presented as means ± SEM. Statistical analysis was performed using two-way ANOVA for multiple group comparisons followed by Bonferroni's correction or Student t test for comparison between two groups. Difference in insulitis score between NOX2$^{-/-}$ and WT mice was analyzed by the χ^2 test. A P value of <0.05 was considered statistically significant.

RESULTS

NOX2 deficiency decreases STZ-induced hyperglycemia. Under normal conditions, adult WT and NOX2$^{-/-}$ mice showed equivalent levels of random blood glucose, serum superoxide, antioxidant, and insulin (Fig. 1). Two days after the final injection of STZ, five of seven WT mice developed hyperglycemia, whereas only one of seven NOX2$^{-/-}$ mice had blood glucose level >11.1 mmol/l. On day 5, all WT mice became diabetic, but there were still two of seven NOX2$^{-/-}$ mice that demonstrated normal blood glucose levels. Compared with WT mice, NOX2$^{-/-}$ mice presented significantly lower random (Fig. 1*A* and *B*) and fasting (Fig. 1*E*) blood glucose levels after STZ treatment ($P < 0.01$). Consistently, the results of IPGTT performed on day 9 as an in vivo measure of β-cell function showed that STZ-induced glucose intolerance was significantly ameliorated in NOX2$^{-/-}$ mice ($P < 0.01$, Fig. 1*C* and *D*). A similar effect was also observed in WT mice treated with an NADPH oxidase inhibitor, apocynin (10 mg/kg body wt/day). In concordance to the blood glucose level results, the serum insulin level was restored in NOX2$^{-/-}$ mice compared with WT mice ($P < 0.05$, Fig. 1*F*). Serum superoxide production significantly increased after STZ treatment in both WT and NOX2$^{-/-}$ mice (Fig. 1*G*). However, compared with WT mice, NOX2$^{-/-}$ mice presented significantly lower serum superoxide levels ($P < 0.01$, Fig. 1*G*). No significant changes were observed in serum antioxidant activity levels or protein expression of antioxidant enzymes including SOD-2 and Gpx1 after STZ treatment (Fig. 1*H*–*J*).

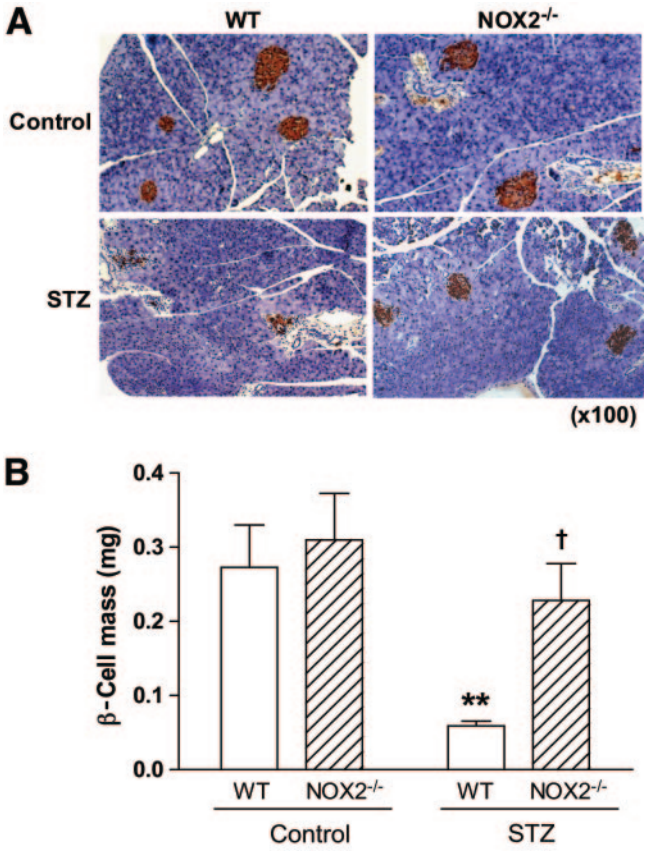

FIG. 3. β-Cell mass after multiple-low-dose STZ treatment. *A*: Representative histological insulin staining of pancreas sections from each experiment group. Insulin-positive cells within islets are stained brown. *B*: No difference in β-cell mass was found between control groups. After STZ treatment, β-cell mass was significantly preserved in NOX2$^{-/-}$ compared with WT mice. Data are means ± SEM; $n = 4–6$ per group. **$P < 0.01$ vs. WT control; †$P < 0.05$ vs. STZ-treated WT. (A high-quality digital representation of this figure is available in the online issue.)

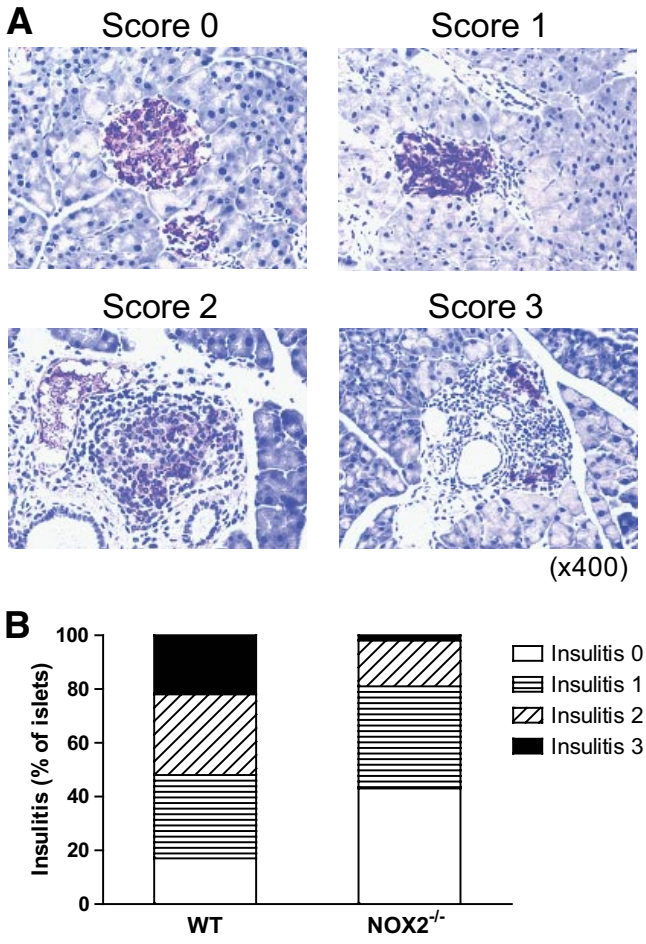

FIG. 4. Islet insulitis after multiple-low-dose STZ treatment. *A*: Representative histological images are shown. The insulitis score was assigned using the following scale: 0, intact islet (A0); 1, peri-insulitis (A1); 2, moderate insulitis (A2, <50% of the islet infiltrated); 3, severe insulitis (A3, ≥50% of the islet infiltrated). *B*: Islets from 10 WT mice and eight NOX2$^{-/-}$ mice were assigned insulitis scores. Less infiltration was found in NOX2$^{-/-}$ islets compared with WT after STZ treatment ($P < 0.01$, χ^2 analysis). Data are means ± SEM. (A high-quality digital representation of this figure is available in the online issue.)

NOX2 deficiency improves β-cell survival after STZ treatment. Apoptosis is an important mechanism in the development of diabetes. We examined β-cell apoptosis 9 days after STZ treatment by transferase-mediated dUTP nick-end labeling (TUNEL) staining and co-staining with insulin. Apoptotic β-cells were detected by immunofluorescence associated with fragmented DNA (Fig. 2*A*). Compared with WT mice, there were significantly less TUNEL-positive β-cells in NOX2$^{-/-}$ mouse islets 9 days after STZ treatment ($P < 0.01$, Fig. 2*B*). Acute cell death in islets after STZ treatment was also investigated. Eight hours after the final STZ injection, a significant decrease in the number of apoptotic and necrotic cells in the islets was observed in NOX2$^{-/-}$ mice compared with WT mice ($P < 0.01$, Fig. 2*C*). Furthermore, necrosis was about 15-fold higher than apoptosis at this early stage of STZ-induced islet damage (Fig. 2*C*).

NOX2 deficiency preserves β-cell mass after STZ treatment. STZ treatment caused destruction of pancreatic β-cells (representative histological images of pancreatic tissue are shown in Fig. 3*A*). In WT mice, the number of functional (insulin immuno-positive) β-cells within islets was markedly decreased as a result of STZ treatment. However, in NOX2$^{-/-}$ mice, β-cells appeared to be protected after the same dose regimen of STZ treatment (Fig. 3*A*). Compared with controls, β-cell mass was significantly decreased in WT mice after STZ treatment ($P < 0.01$). However, NOX2 deficiency significantly preserved the β-cell mass ($P < 0.05$, Fig. 3*B*).

NOX2 deficiency attenuated islet insulitis after STZ treatment. Insulitis is an important process in β-cell destruction induced by STZ. A scoring system was used to evaluate the extent of insulitis after STZ treatment. An example of each score grade was shown in Fig. 4*A*. Histological analysis showed the presence of insulitis in both groups of mice, with significant differences in the degree of leukocyte infiltration ($P < 0.01$). In NOX2$^{-/-}$ mice, 43% of islets exhibited no insulitis, with 38% of islets showing only peri-insulitis. However, in WT mice, half of the islets showed grade 2–3 insulitis (Fig. 4*B*).

NOX2 deficiency improves islet function and decreases ROS production during cytokine treatment in vitro. Islets isolated from WT and NOX2$^{-/-}$ mice showed a similar level of insulin release in response to glucose stimulation (Fig. 5*A*). The cytokine treatment (2 ng/ml each of IL-1β, IFN-γ, and TNF-α) significantly decreased insulin release from the WT islets ($P < 0.01$). However, this impairment was abrogated in NOX2$^{-/-}$ islets ($P < 0.01$, Fig. 5*A*). Cytokine treatment significantly increased

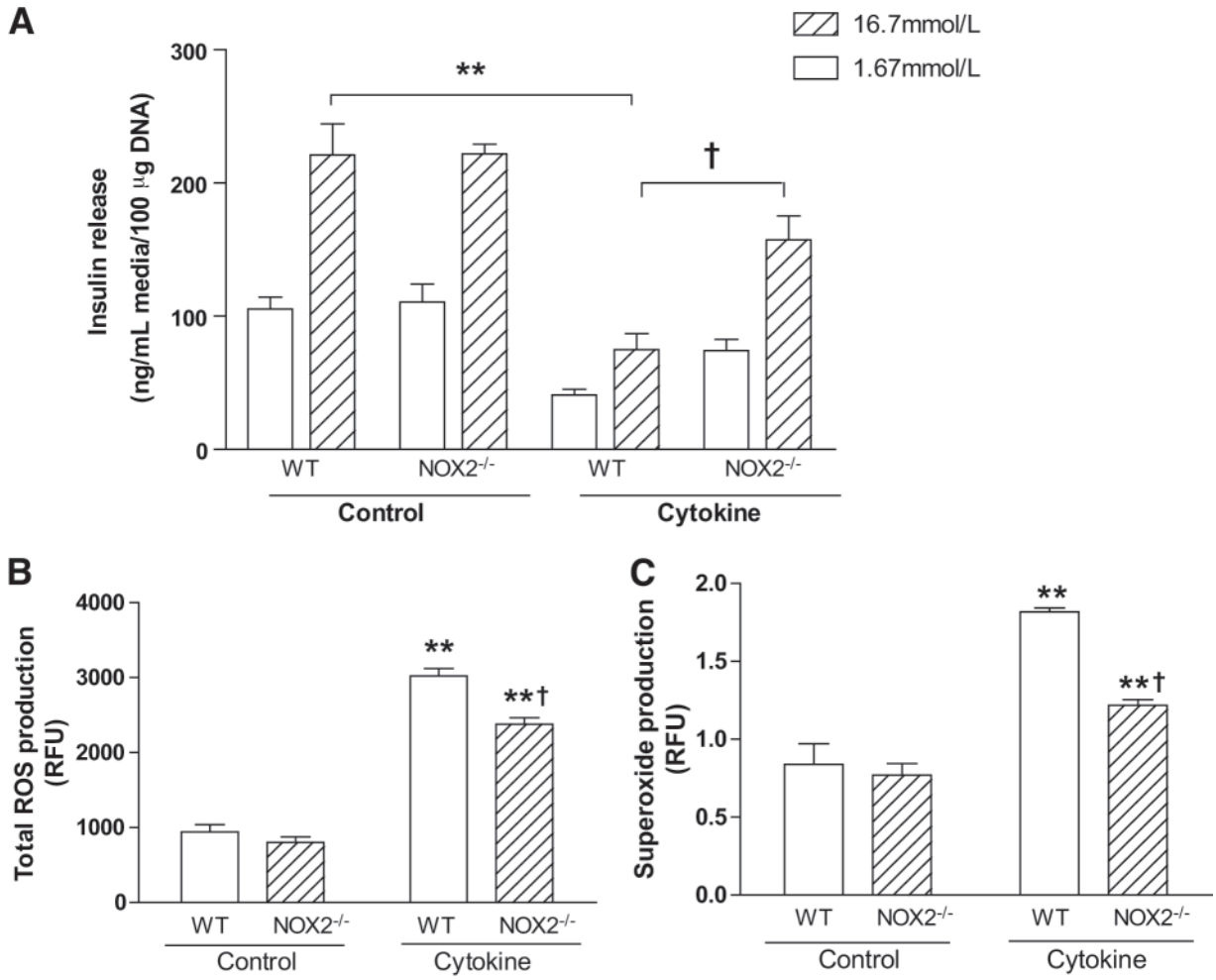

FIG. 5. Isolated islet function and ROS production after cytokine treatment. *A*: Glucose-stimulated insulin release after treatment with combined cytokines for 48 h. Insulin release in response to 16.7 mmol/l glucose was significantly impaired in cytokine-treated isolated WT islets compared with WT control but was well preserved in cytokine-treated NOX2$^{-/-}$ islets. *B*: Total ROS production detected by dichlorofluorescein diacetate in isolated islets treated with cytokines. After cytokine treatment, ROS in the islets significantly increased compared with control groups. NOX2$^{-/-}$ islets showed a significantly lower ROS production compared with WT. *C*: Superoxide production detected by dihydroethidium in isolated islets treated with cytokines. After cytokine treatment, superoxide production in the islets was significantly increased compared with control groups. NOX2$^{-/-}$ islets showed a significantly lower superoxide production compared with WT. Data are means ± SEM; n = 4–5 per group. **P < 0.01 vs. WT control; †P < 0.01 vs. cytokine-treated WT. RFU, relative fluorescence unit.

total ROS and superoxide production in both WT and NOX2$^{-/-}$ islets ($P < 0.01$). When compared with WT, both total ROS (Fig. 5*B*) and superoxide (Fig. 5*C*) levels of NOX2$^{-/-}$ islets were significantly decreased ($P < 0.01$).

NOX2 deficiency of the immune system decreases STZ-induced hyperglycemia. Adoptive transfer was used to replace the WT immune environment with a NOX2-deficient one. Five weeks after adoptive transfer, basal blood glucose levels of WT^{WT} and WT$^{NOX2-/-}$ mice remained normal. STZ treatment induced a severe hyperglycemia in WT^{WT} mice. However, the WT$^{NOX2-/-}$ mice demonstrated a significantly lower level of random blood glucose (Fig. 6*A* and *B*, $P < 0.01$) and fasting blood glucose (Fig. 6*E*, $P < 0.01$), higher serum insulin level (Fig. 6*F*, $P < 0.01$), and less intolerance to IPGTT compared with WT^{WT} (Fig. 6*C* and *D*, $P < 0.05$). WT and NOX2$^{-/-}$ splenocytes used to perform the adoptive transfer were stimulated with ConA. Superoxide production detected by lucigenin assay in response to ConA stimulation was significantly attenuated in NOX2$^{-/-}$ splenocytes compared with WT ($P < 0.01$, Fig. 6*G*). Moreover, 48 h after ConA stimulation, the proinflammatory cytokine release (TNF-α and IL-1β) was significantly impaired in NOX2$^{-/-}$ splenocytes compared with WT ($P < 0.05$, Fig. 6*H* and *I*).

NOX2 deficiency prevents alloxan-induced diabetes. After alloxan treatment (60 mg/kg i.v.), all WT mice developed hyperglycemia, whereas none of the NOX2$^{-/-}$ mice had blood glucose levels >11.1 mmol/l on day 2 and 5. NOX2$^{-/-}$ mice presented significantly lower random (Fig. 7*A* and *B*) and fasting (Fig. 7*E*) blood glucose levels compared with WT ($P < 0.01$). Consistently, IPGTT performed on day 9 showed that alloxan-induced glucose intolerance was abrogated in NOX2$^{-/-}$ mice ($P < 0.01$, Fig. 7*C* and *D*). Furthermore, serum insulin levels were significantly increased in NOX2$^{-/-}$ compared with WT mice after alloxan treatment ($P < 0.01$, Fig. 7*F*).

DISCUSSION

In the present study, we demonstrated for the first time that deficiency of NOX2 protects against the onset and development of STZ-induced diabetes in mice. STZ-induced hyperglycemia was significantly inhibited in NOX2$^{-/-}$ compared with WT mice. In agreement with the

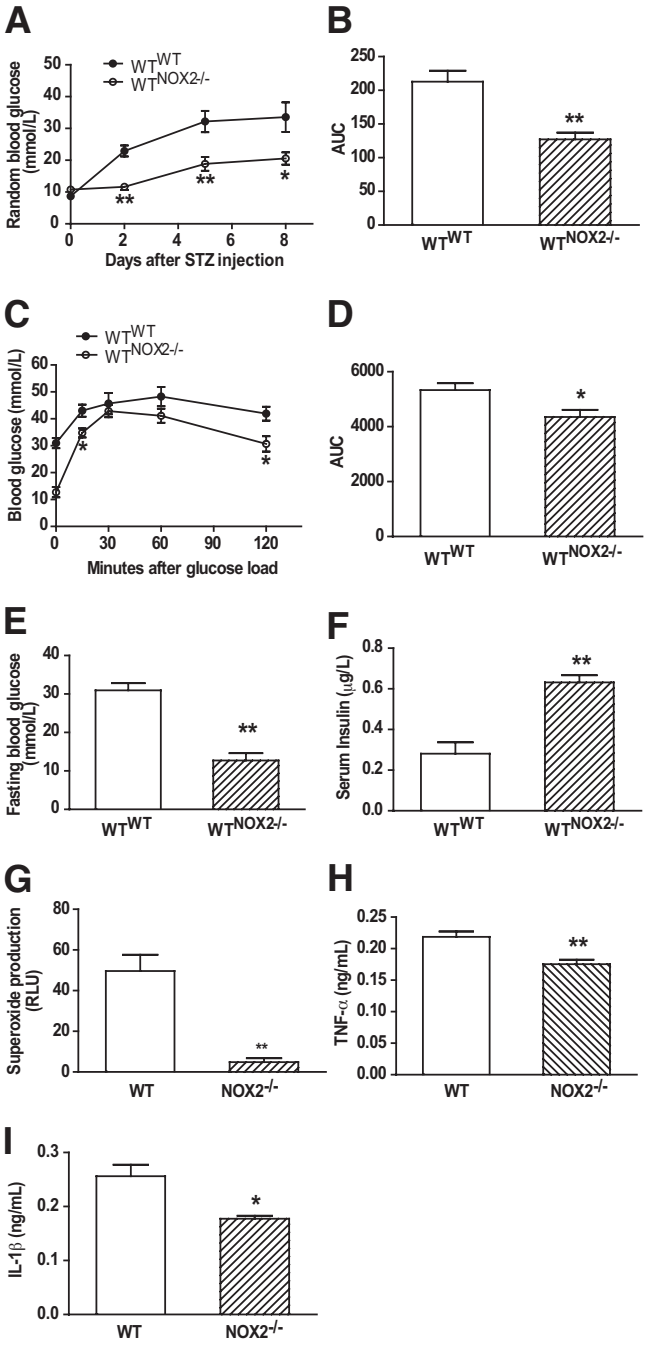

FIG. 6. Effects of adoptive transfer with NOX2$^{-/-}$ splenocytes on β-cell function after multiple-low-dose STZ treatment. *A–F*: Blood glucose and insulin levels after STZ treatment in mice that underwent adoptive transfer. WT$^{NOX2-/-}$ and WT^{WT} indicate WT mice adoptively transferred with NOX2$^{-/-}$ and WT splenocytes, respectively. The WT$^{NOX2-/-}$ mice showed lower random (*A* and *B*) and fasting (*E*) blood glucose levels and higher serum insulin level (*F*) than WT^{WT} mice after STZ treatment. IPGTT results (*C* and *D*) demonstrated that the in vivo β-cell function of WT$^{NOX2-/-}$ mice was significantly preserved when compared with WT^{WT} mice after STZ treatment. *$P < 0.05$, **$P < 0.01$ vs. WT^{WT}. *G–I*: The ability of NOX2$^{-/-}$ splenocytes to produce ROS (*G*) and proinflammatory cytokines, TNF-α (*H*) and IL-1β (*I*), in response to ConA (5 μg/ml) simulation was significantly impaired compared with WT splenocytes. *$P < 0.05$, **$P < 0.01$ vs. WT. Data are means ± SEM; $n = 4–6$ per group. AUC, area under the curve; RLU, relative luminescence unit.

blood glucose levels, the in vivo islet function measured by IPGTT and the serum insulin levels after STZ treatment were restored in NOX2$^{-/-}$ mice. Histological investigation of pancreatic tissue revealed that the majority of β-cells in WT pancreatic islets was destroyed by the STZ, whereas the β-cell mass was well preserved in NOX2$^{-/-}$ mice. These data clearly showed the protective effects of NOX2 deficiency against STZ-induced diabetes, suggesting a critical role of NOX2-containing NADPH oxidase in β-cell destruction in diabetes.

In the multiple-low-dose STZ model, diabetes is induced by two main mechanisms (3,26,27). One is the direct cytotoxic effect of STZ on β-cells by alkylation of nuclear and mitochondrial DNA. The other is the local infiltration in the pancreatic islets and inflammation by mononuclear cells including lymphocytes and macrophages, which simulate the autoimmune reaction in type 1 diabetes (28). Although ROS has been implicated in both mechanisms, the source of the ROS production during development of diabetes is still not clear. Recently, functional phagocyte-like NADPH oxidase has been found in T-cells (17) and β-cells (18). NOX has been shown to be quantitatively an important source of ROS in pancreatic islets (18,29). In the present study, cell death at 8 h after the third STZ treatment was significantly decreased in the NOX2$^{-/-}$ mice. Although cytokine (IL-1β, IFN-γ, and TNF-α) treatment significantly increased total ROS and superoxide production of the WT islets, both total ROS and superoxide levels were significantly decreased in the NOX2$^{-/-}$ islets. Furthermore, β-cell function in terms of insulin release was well preserved in NOX2$^{-/-}$ islets. Additionally, serum insulin levels and IPGTT were restored in NOX2$^{-/-}$ mice after STZ treatment in vivo. These data suggest that NOX2-containing NADPH oxidase plays an important role not only in the early islet cell death from STZ, but also cytokine-mediated ROS production in the islets leading to impairment of β-cell function.

Alloxan is another diabetogenic chemical used frequently because of its ability to selectively damage β-cells by inducing ROS formation (3). To further demonstrate that decreased ROS production due to NOX2 deficiency protects against diabetes, the alloxan diabetes model was used. Results showed that NOX2 deficiency prevented diabetes development after alloxan treatment. Our data provide convincing evidence for an important role of NOX2-mediated ROS production in diabetes development.

Type 1 diabetes is an autoimmune disease. Activation and recruitment of immune cells including β-cell–specific CD8$^+$ T-cells have been implicated in the pathogenesis of diabetes through cytokine expression and ROS production leading to β-cell destruction (1). In fact, recent studies have shown that T-cells have functional NADPH oxidase enzyme, and deficiency in NOX2 decreases their ability to produce ROS according to antigen stimulation (17). In the present study, we isolated splenocytes and measured ConA-stimulated superoxide production and proinflammatory cytokine release, which reflects immune cell activation. Our data showed that superoxide production and proinflammatory cytokine release (TNF-α and IL-1β) were significantly decreased in NOX2-deficient splenocytes. To further investigate the contribution of NOX2 in immune cells to functional impairment and damage of β-cells, NOX2$^{-/-}$ splenocytes were adoptively transferred into lethally irradiated WT mice to reproduce the altered immune system in the NOX2 animals. Consistent with our hypothesis, a significantly lower blood glucose level, higher serum insulin level, and better islet function were observed in the WT mice repopulated with NOX2 splenocytes compared with the control group after STZ treat-

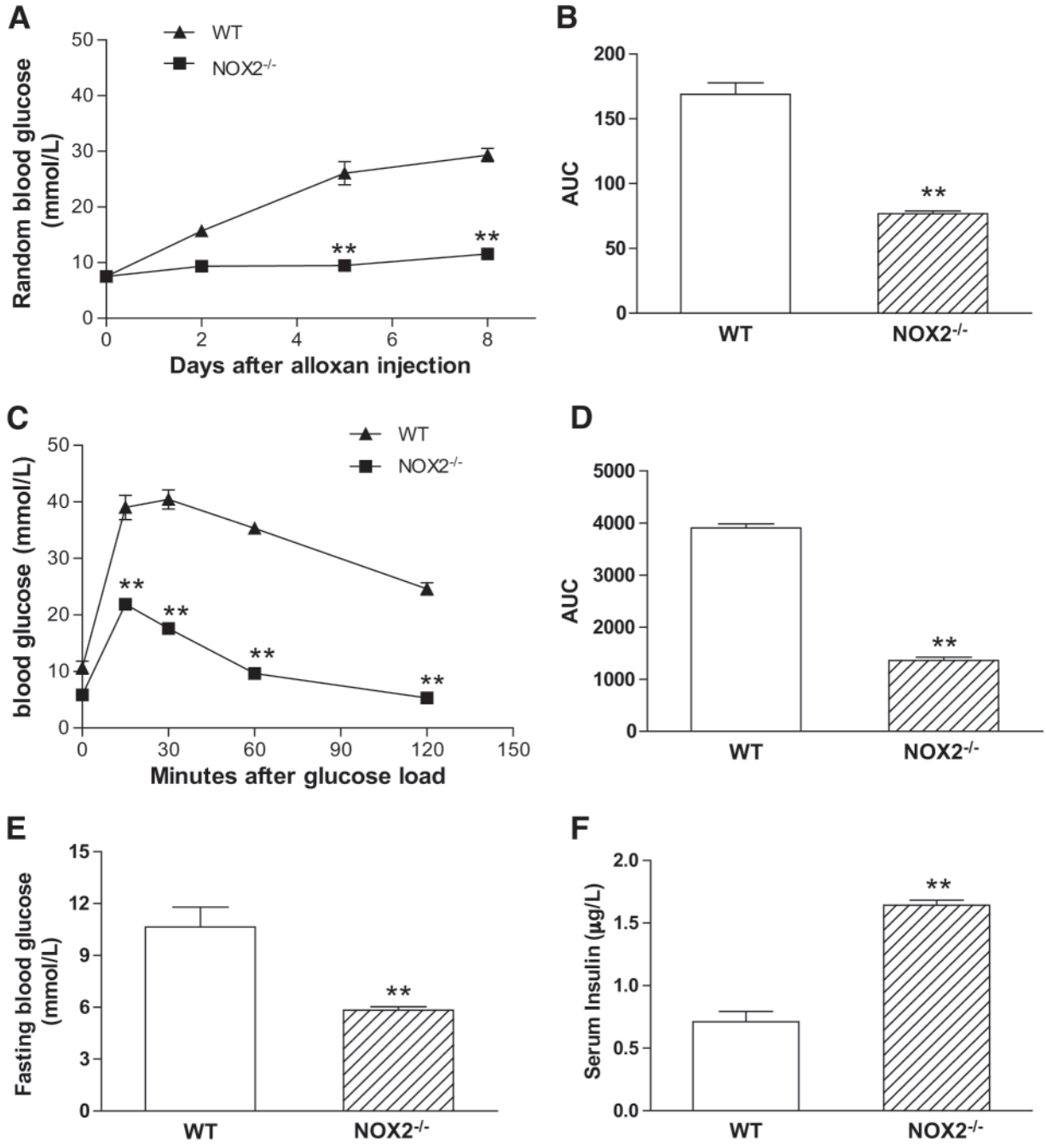

FIG. 7. Blood glucose and serum insulin levels after alloxan treatment. *A* and *B*: NOX2$^{-/-}$ mice showed significant decreased random blood glucose levels compared with WT after alloxan treatment. *C* and *D*: An IPGTT at 9 days after alloxan treatment revealed that β-cell function was significantly better in NOX2$^{-/-}$ mice than in WT mice. *E* and *F*: NOX2$^{-/-}$ mice had a significantly lower fasting blood glucose level and higher serum insulin levels than WT mice after alloxan treatment. Data are means ± SEM; $n = 6$ per group. **$P < 0.01$ vs. WT. AUC, area under the curve.

ment. Our results suggest that NOX2-containing NADPH oxidase in the activated immune cells including T-cells also plays a key role in the impairment of islet function after STZ treatment.

In type 1 diabetes and animal models of STZ-induced diabetes, leukocytic infiltration (insulitis) and the production of proinflammatory cytokines contribute significantly to β-cell destruction (30–32). Infiltrated macrophages and T-cells generate cytotoxic mediators including cytokines and induce β-cell death through apoptosis (33,34). In our study, decreased insulitis and apoptosis were observed in the islets of NOX2$^{-/-}$ mice, leading to the well-preserved β-cell mass after STZ treatment, which can be explained by a reduction of early islet cell death and the decreased ability of NOX2$^{-/-}$ splenocytes to produce superoxide and release proinflammatory cytokines. Previous studies have also shown that NOX2 deficiency results in decreased superoxide production from polymorphonuclear neutrophils and macrophages (34) and decreased hydrogen peroxide generation from T-cells (17). Antigen-presenting cells deficient in NOX2 have an impaired ability to present antigens due to enhanced antigen degradation (35). Additionally, the peripheral blood memory B lymphocyte compartment is reduced in patients with chronic granulo-

matous disease, which mainly results from NOX2 deficiency (36). Taken together, NOX2 deficiency protects against β-cell destruction and preserves islet function in the STZ-induced diabetes by inhibiting insulitis. These beneficial effects are likely due to less early β-cell death from toxic effects of STZ and an inhibition of immune reaction, including decreased antigen presentation, impaired immune cell activation, and suppression of cytotoxic effects from T-cells, neutrophils, and macrophages during development of diabetes.

In conclusion, our study demonstrated that NOX2 deficiency attenuates the severity of hyperglycemia, β-cell mass loss, and insulitis in the multiple-low-dose STZ-induced diabetes in mice. The protective effects are a result of decreased β-cell apoptosis, decreased ROS production from the islets, and suppressed immune response. The ability of NOX2 in regulating the immune response in this model supports an important role of NOX2-containing NADPH oxidase in the development of diabetes induced by STZ. NOX2 may represent a potential therapeutic target for treatment of diabetes.

ACKNOWLEDGMENTS

This study was supported by grants from the Canadian Institutes of Health Research (MOP-14653 to Q.F.) and the Heart and Stroke Foundation of Ontario (HSFO) (T-6040 to Q.F.). F.-L.X. was supported by a Doctoral Research Award from the Heart and Stroke Foundation of Canada. Q.F. is an HSFO Career Investigator.

No potential conflicts of interest relevant to this article were reported.

F.-L.X. researched data and wrote the manuscript. X.L. reviewed/edited the manuscript. B.S. researched data. D.J.H. reviewed/edited the manuscript. Q.F. wrote the manuscript.

REFERENCES

1. Yoon JW, Jun HS. Autoimmune destruction of pancreatic beta cells. Am J Ther 2005;12:580–591
2. Masutani M, Suzuki H, Kamada N, Watanabe M, Ueda O, Nozaki T, Jishage K, Watanabe T, Sugimoto T, Nakagama H, Ochiya T, Sugimura T. Poly(ADP-ribose) polymerase gene disruption conferred mice resistant to streptozotocin-induced diabetes. Proc Natl Acad Sci U S A 1999;96:2301–2304
3. Lenzen S. The mechanisms of alloxan- and streptozotocin-induced diabetes. Diabetologia 2008;51:216–226
4. Mathews CE, Suarez-Pinzon WL, Baust JJ, Strynadka K, Leiter EH, Rabinovitch A. Mechanisms underlying resistance of pancreatic islets from ALR/Lt mice to cytokine-induced destruction. J Immunol 2005;175:1248–1256
5. Harmon JS, Bogdani M, Parazzoli SD, Mak SS, Oseid EA, Berghmans M, Leboeuf RC, Robertson RP. Beta-cell-specific overexpression of glutathione peroxidase preserves intranuclear MafA and reverses diabetes in db/db mice. Endocrinology 2009;150:4855–4862
6. Kubisch HM, Wang J, Bray TM, Phillips JP. Targeted overexpression of Cu/Zn superoxide dismutase protects pancreatic beta-cells against oxidative stress. Diabetes 1997;46:1563–1566
7. Chen H, Carlson EC, Pellet L, Moritz JT, Epstein PN. Overexpression of metallothionein in pancreatic beta-cells reduces streptozotocin-induced DNA damage and diabetes. Diabetes 2001;50:2040–2046
8. Azevedo-Martins AK, Lortz S, Lenzen S, Curi R, Eizirik DL, Tiedge M. Improvement of the mitochondrial antioxidant defense status prevents cytokine-induced nuclear factor-kappaB activation in insulin-producing cells. Diabetes 2003;52:93–101
9. Lortz S, Tiedge M, Nachtwey T, Karlsen AE, Nerup J, Lenzen S. Protection of insulin-producing RINm5F cells against cytokine-mediated toxicity through overexpression of antioxidant enzymes. Diabetes 2000;49:1123–1130
10. Tiedge M, Lortz S, Munday R, Lenzen S. Protection against the co-operative toxicity of nitric oxide and oxygen free radicals by overexpression of antioxidant enzymes in bioengineered insulin-producing RINm5F cells. Diabetologia 1999;42:849–855
11. Hotta M, Tashiro F, Ikegami H, Niwa H, Ogihara T, Yodoi J, Miyazaki J. Pancreatic beta cell-specific expression of thioredoxin, an antioxidative and antiapoptotic protein, prevents autoimmune and streptozotocin-induced diabetes. J Exp Med 1998;188:1445–1451
12. Xu B, Moritz JT, Epstein PN. Overexpression of catalase provides partial protection to transgenic mouse beta cells. Free Radic Biol Med 1999;27:830–837
13. Newsholme P, Morgan D, Rebelato E, Oliveira-Emilio HC, Procopio J, Curi R, Carpinelli A. Insights into the critical role of NADPH oxidase(s) in the normal and dysregulated pancreatic beta cell. Diabetologia 2009;52:2489–2498
14. Babior BM, Lambeth JD, Nauseef W. The neutrophil NADPH oxidase. Arch Biochem Biophys 2002;397:342–344
15. Lambeth JD. NOX enzymes and the biology of reactive oxygen. Nat Rev Immunol 2004;4:181–189
16. Segal AW. How neutrophils kill microbes. Annu Rev Immunol 2005;23:197–223
17. Jackson SH, Devadas S, Kwon J, Pinto LA, Williams MS. T cells express a phagocyte-type NADPH oxidase that is activated after T cell receptor stimulation. Nat Immunol 2004;5:818–827
18. Oliveira HR, Verlengia R, Carvalho CR, Britto LR, Curi R, Carpinelli AR. Pancreatic beta-cells express phagocyte-like NAD(P)H oxidase. Diabetes 2003;52:1457–1463
19. Calcinaro F, Dionisi S, Marinaro M, Candeloro P, Bonato V, Marzotti S, Corneli RB, Ferretti E, Gulino A, Grasso F, De Simone C, Di Mario U, Falorni A, Boirivant M, Dotta F. Oral probiotic administration induces interleukin-10 production and prevents spontaneous autoimmune diabetes in the non-obese diabetic mouse. Diabetologia 2005;48:1565–1575
20. Feng Q, Song W, Lu X, Hamilton JA, Lei M, Peng T, Yee SP. Development of heart failure and congenital septal defects in mice lacking endothelial nitric oxide synthase. Circulation 2002;106:873–879
21. Cardinal JW, Margison GP, Mynett KJ, Yates AP, Cameron DP, Elder RH. Increased susceptibility to streptozotocin-induced beta-cell apoptosis and delayed autoimmune diabetes in alkylpurine-DNA-N-glycosylase-deficient mice. Mol Cell Biol 2001;21:5605–5613
22. Fujita H, Kakei M, Fujishima H, Morii T, Yamada Y, Qi Z, Breyer MD. Effect of selective cyclooxygenase-2 (COX-2) inhibitor treatment on glucose-stimulated insulin secretion in C57BL/6 mice. Biochem Biophys Res Commun 2007;363:37–43
23. Flodström M, Tyrberg B, Eizirik DL, Sandler S. Reduced sensitivity of inducible nitric oxide synthase-deficient mice to multiple low-dose streptozotocin-induced diabetes. Diabetes 1999;48:706–713
24. Robinson KM, Janes MS, Pehar M, Monette JS, Ross MF, Hagen TM, Murphy MP, Beckman JS. Selective fluorescent imaging of superoxide in vivo using ethidium-based probes. Proc Natl Acad Sci U S A 2006;103:15038–15043
25. Peng T, Lu X, Feng Q. Pivotal role of gp91phox-containing NADH oxidase in lipopolysaccharide-induced tumor necrosis factor-alpha expression and myocardial depression. Circulation 2005;111:1637–1644
26. Paik SG, Fleischer N, Shin SI. Insulin-dependent diabetes mellitus induced by subdiabetogenic doses of streptozotocin: obligatory role of cell-mediated autoimmune processes. Proc Natl Acad Sci U S A 1980;77:6129–6133
27. Bonnevie-Nielsen V, Steffes MW, Lernmark A. A major loss in islet mass and B-cell function precedes hyperglycemia in mice given multiple low doses of streptozotocin. Diabetes 1981;30:424–429
28. Like AA, Rossini AA. Streptozotocin-induced pancreatic insulitis: new model of diabetes mellitus. Science 1976;193:415–417
29. Morgan D, Oliveira-Emilio HR, Keane D, Hirata AE, Santos da Rocha M, Bordin S, Curi R, Newsholme P, Carpinelli AR. Glucose, palmitate and pro-inflammatory cytokines modulate production and activity of a phagocyte-like NADPH oxidase in rat pancreatic islets and a clonal beta cell line. Diabetologia 2007;50:359–369
30. Fukuda K, Tesch GH, Yap FY, Forbes JM, Flavell RA, Davis RJ, Nikolic-Paterson DJ. MKK3 signalling plays an essential role in leukocyte-mediated pancreatic injury in the multiple low-dose streptozotocin model. Lab Invest 2008;88:398–407
31. Hohmeier HE, Tran VV, Chen G, Gasa R, Newgard CB. Inflammatory mechanisms in diabetes: lessons from the beta-cell. Int J Obes Relat Metab Disord 2003;27(Suppl. 3):S12–S16
32. Kawasaki E, Abiru N, Eguchi K. Prevention of type 1 diabetes: from the view point of beta cell damage. Diabetes Res Clin Pract 2004;66(Suppl. 1):S27–S32
33. Mellado-Gil JM, Aguilar-Diosdado M. High glucose potentiates cytokine-

and streptozotocin-induced apoptosis of rat islet cells: effect on apoptosis-related genes. J Endocrinol 2004;183:155–162
34. Ostanin DV, Barlow S, Shukla D, Grisham MB. NADPH oxidase but not myeloperoxidase protects lymphopenic mice from spontaneous infections. Biochem Biophys Res Commun 2007;355:801–806
35. Savina A, Jancic C, Hugues S, Guermonprez P, Vargas P, Moura IC, Lennon-Duménil AM, Seabra MC, Raposo G, Amigorena S. NOX2 controls phagosomal pH to regulate antigen processing during crosspresentation by dendritic cells. Cell 2006;126:205–218
36. Bleesing JJ, Souto-Carneiro MM, Savage WJ, Brown MR, Martinez C, Yavuz S, Brenner S, Siegel RM, Horwitz ME, Lipsky PE, Malech HL, Fleisher TA. Patients with chronic granulomatous disease have a reduced peripheral blood memory B cell compartment. J Immunol 2006;176:7096–7103